(η^2-*trans*-Cyclooctene)$_2$Fe(CO)$_3$ and Related Complexes: Structure and Dynamic Behavior

Hildegard Angermund, Friedrich-Wilhelm Grevels,* and Rainer Moser

Max-Planck-Institut für Strahlenchemie, D-4330 Mülheim a.d. Ruhr, Federal Republic of Germany

Reinhard Benn, Carl Krüger, and Maria J. Romão

Max-Planck-Institut für Kohlenforschung, D-4330 Mülheim a.d. Ruhr, Federal Republic of Germany

Received December 23, 1987

(η^2-*trans*-Cyclooctene)(η^2-olefin)Fe(CO)$_3$ complexes are synthesized by thermal olefin exchange [**3**, olefin = *trans*-cyclooctene, from (η^2-*cis*-cyclooctene)$_2$Fe(CO)$_3$ (**2**) and *trans*-cyclooctene; **6**, olefin = methyl acrylate, from (η^2-methyl acrylate)$_2$Fe(CO)$_3$ and *trans*-cyclooctene] or CO photosubstitution [**3**, from Fe(CO)$_5$ and excess *trans*-cyclooctene; **5**, olefin = dimethyl fumarate, from (η^2-*trans*-cyclooctene)Fe(CO)$_4$ and dimethyl fumarate or from (η^2-dimethyl fumarate)Fe(CO)$_4$ and *trans*-cyclooctene]. The products are obtained as mixtures of diastereomers, some of which (**3a**, C_2 isomer; **3b**, C_s isomer; **5a**) are separated by fractional crystallization. The reaction of **2** with (−)-*trans*-cyclooctene yields (−)-**3a**. Single-crystal X-ray diffraction analyses of racemic **3a** and **5a** establish a trigonal-bipyramidal geometry with the C=C units occupying two equatorial positions. Crystals of racemic **3a** are monoclinic of space group $P2_1/n$ with a = 12.069 (2) Å, b = 8.278 (1) Å, c = 18.815 (2) Å, β = 98.386 (9)°, and Z = 4. The unit cell contains two molecules of each **3a** enantiomer. The structure was solved and refined to R = 0.034 and R_w = 0.037 by using 4218 independent reflections. Crystals of **5a** are orthorhombic of space group $P2_12_12_1$ with a = 7.811 (1) Å, b = 13.167 (1) Å, c = 20.432 (2) Å, and Z = 4. The structure was solved and refined to R = 0.037 and R_w = 0.045 by using 5506 independent reflections. All compounds are characterized by elemental analysis and IR (including CO force field parameters of **3a**) and ^{13}C NMR spectroscopy. The ^{13}C NMR coordination shifts of the olefinic carbon atoms in **3a** and **5a** correlate (inversely) with the respective metal–carbon distances. Variable-temperature ^{13}C NMR spectroscopy of **3b** reveals three sequential dynamic processes: (a) olefin rotation ($\Delta H^\ddagger$ = 8.0 ± 0.5 kcal mol^{-1}, $\Delta S^\ddagger$ = −5.1 ± 3 cal mol^{-1} K^{-1}), (b) eq-CO/ax-CO two-site exchange ($\Delta H^\ddagger$ = 13.8 ± 0.4 kcal mol^{-1}, $\Delta S^\ddagger$ = 2.8 ± 1.2 cal mol^{-1} K^{-1}), (c) complete CO scrambling ($\Delta H^\ddagger$ = 16.8 ± 0.8 kcal mol^{-1}, $\Delta S^\ddagger$ = 10.2 ± 3 cal mol^{-1} K^{-1}). In the case of **3a** the two CO site-exchange processes are indistinguishable. The dynamic behavior of the mixed bis(olefin) complexes **5a** and **6** indicates that the two olefins rotate independently, and rotation of both of the olefins appears to be a prerequisite for CO scrambling. In conclusion, these observations are in accord with a sequence of three Berry pseudorotational steps, alternately using an olefin, a CO group, and the respective other olefin as the pivotal ligand.

Introduction

Mono- and diolefin carbonyliron complexes[1,2] of types (η^2-monoolefin)Fe(CO)$_4$ and (η^4-diolefin)Fe(CO)$_3$ have been thoroughly investigated with regard to synthetic, structural, and spectroscopic aspects. By contrast, tricarbonyliron complexes with two monoolefinic ligands, (η^2-monoolefin)$_2$Fe(CO)$_3$, are far less well-documented, although such compounds are considered to be involved as relevant intermediates in processes such as carbonyliron-catalyzed olefin isomerization[3–5] and olefin coupling reactions.[6,7] Only two complexes of this type, with methyl acrylate[8] and *cis*-cyclooctene[4] as the olefinic ligands, have been isolated in pure state. (η^2-Ethene)$_2$Fe(CO)$_3$[5,9] and other labile (η^2-alkene)$_2$Fe(CO)$_3$ derivatives[5] were photochemically generated in solution,[5] in hydrocarbon glasses,[5] or in the gas phase[9] and characterized by infrared[5,9] and NMR[5] spectroscopy. In all cases the CO stretching vibrational pattern is distinctly different from those of typical square-pyramidal (η^4-diolefin)Fe(CO)$_3$ complexes; it rather indicates a trigonal-bipyramidal structure with two equatorially coordinated olefinic double bonds, analogous to the unique, nonconjugated diolefin complex (η^2,η^2-1,5-dimethylene-2,6-dimethylcyclooctane)Fe(CO)$_3$ (**1**).[10] The lability in solution of the aforesaid (η^2-monoolefin)$_2$Fe(CO)$_3$ complexes is a particular advantage with respect to their application as a source of the Fe(CO)$_3$ unit.[4,5] On the other hand, it seriously hampers further spectroscopic studies on these compounds. Not even crystals suitable for X-ray crystallography could be obtained.

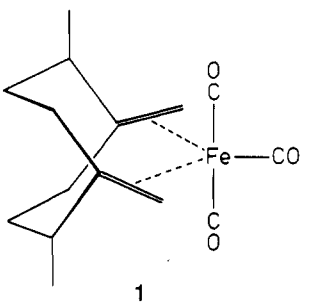

1

On that account it was desirable to find more stable representatives of this class of compounds. *trans*-Cyclooctene has been reported to form stable complexes with a variety of transition metals.[11–15] Therefore, this olefin

(1) Koerner von Gustorf, E. A.; Grevels, F.-W.; Fischler, I., Eds. *The Organic Chemistry of Iron*; Academic: New York, 1978; Vol. 1.
(2) Deeming, A. J. In *Comprehensive Organometallic Chemistry*; Wilkinson, G., Stone, F. G. A., Abel, E. W., Eds.; Pergamon: Oxford, 1982; Vol. 4, p 377.
(3) Schroeder, M. A.; Wrighton, M. S. *J. Am. Chem. Soc.* **1976**, *98*, 551.
(4) Fleckner, H.; Grevels, F.-W.; Hess, D. *J. Am. Chem. Soc.* **1984**, *106*, 2027.
(5) Wuu, Y.-M.; Bentsen, J. G.; Brinkley, C. G.; Wrighton, M. S. *Inorg. Chem.* **1987**, *26*, 530.
(6) Weissberger, E.; Laszlo, P. *Acc. Chem. Res.* **1976**, *9*, 209.
(7) Stockis, A.; Hoffmann, R. *J. Am. Chem. Soc.* **1980**, *102*, 2952.
(8) Grevels, F.-W.; Schulz, D.; Koerner von Gustorf, E. *Angew. Chem.* **1974**, *86*, 558; *Angew. Chem., Int. Ed. Engl.* **1974**, *13*, 534.
(9) Weiller, B. H.; Miller, M. E.; Grant, E. R. *J. Am. Chem. Soc.* **1987**, *109*, 352.
(10) Grevels, F.-W.; Schneider, K.; Krüger, C.; Goddard, R. *Z. Naturforsch., B*: **1980**, *35*, 360.
(11) Cope, A. C.; Pike, R. A.; Spencer, C. F. *J. Am. Chem. Soc.* **1953**, *75*, 3212.

0276-7333/88/2307-1994$01.50/0

was the first choice for an attempt at the synthesis of a stable (η^2-olefin)$_2$Fe(CO)$_3$ complex.

Results

(η^2-*trans*-Cyclooctene)$_2$Fe(CO)$_3$ (3). Tricarbonylbis(η^2-*trans*-cyclooctene)iron (3) is readily available from the reaction of (η^2-*cis*-cyclooctene)$_2$Fe(CO)$_3$ (2)[4] with *trans*-cyclooctene (eq 1). Olefin exchange is completed

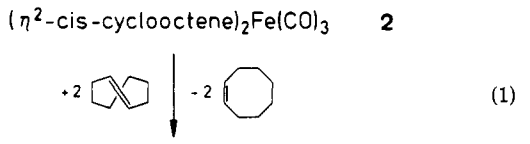

(1)

within a few minutes upon warming a cold solution of **2** and *trans*-cyclooctene in *n*-hexane or diethyl ether to room temperature and results in a nearly quantitative yield of **3**.

Complex **3** is also accessible from the photoreaction of pentacarbonyliron with *trans*-cyclooctene. This route (eq 2) involves the initial formation of (η^2-*trans*-cyclooctene)Fe(CO)$_4$ (**4**)[13] which upon further irradiation is converted into the final product **3**.[16]

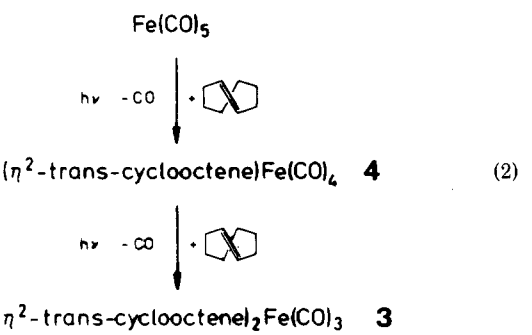

(2)

Either of the two routes, eqs 1 or 2, yields **3** as a mixture of two isomers that can be separated by repetitive fractional crystallization from *n*-hexane or diethyl ether. The less soluble isomer is designated **3a** and the other one **3b**. The infrared CO stretching vibrational bands of the two complexes are almost identical with respect to frequencies as well as relative intensities, thus indicating analogous coordination geometries. The observed pattern (Figure 1) suggests a trigonal-bipyramidal structure in which the olefinic ligands occupy two equatorial positions.

Structure of 3a. With a trans-1,2-disubstituted olefin such as *trans*-cyclooctene two different (η^2-olefin)$_2$Fe(CO)$_3$ complexes of this type are possible: one with C_2 symmetry and one with C_s symmetry. Formation of the C_s isomer involves both of the two enantiomers of *trans*-cyclooctene, whereas in each molecule of the C_2 isomer only one of the *trans*-cyclooctene enantiomers is present. Accordingly, racemic *trans*-cyclooctene yields a mixture of the C_s and racemic C_2 complexes (ca. 1:1), whereas the olefin exchange of **2** (eq 1) with pure (−)-*trans*-cyclooctene[12] yields only one product, the optically active C_2 complex. This reaction may serve as a test for the enantiomeric purity of the chiral olefin. Contamination of (−)-*trans*-cyclooctene with the optical antipode is immediately recognized by the appearance of the C_s isomer in addition to the C_2 (η^2-*trans*-cyclooctene)$_2$Fe(CO)$_3$ complex, as monitored by ^{13}C NMR spectroscopy of the crude product. The chiral C_2 complex was proven by NMR spectroscopy to be identical with **3a**. Consequently, the C_s structure has to be assigned to the other isomer **3b**.

These conclusions have been confirmed by an X-ray structure analysis of racemic **3a** (Figure 2; Tables I–III). As expected and in accord with a variety of (η^2-olefin)-

Table I. Selected Bond Distances (Å) in 3a

Fe–C1	1.796 (3)	C6–C7	1.535 (4)
Fe–C2	1.809 (3)	C7–C8	1.531 (5)
Fe–C3	1.800 (2)	C8–C9	1.544 (5)
Fe–C4	2.128 (2)	C9–C10	1.533 (5)
Fe–C5	2.131 (2)	C10–C11	1.534 (4)
Fe–C12	2.130 (2)	C12–C13	1.404 (3)
Fe–C13	2.123 (2)	C12–C19	1.499 (4)
O1–C1	1.140 (3)	C13–C14	1.505 (4)
O2–C2	1.143 (3)	C14–C15	1.535 (4)
O3–C3	1.142 (3)	C15–C16	1.527 (4)
C4–C5	1.394 (3)	C16–C17	1.546 (5)
C4–C11	1.505 (4)	C17–C18	1.535 (5)
C5–C6	1.508 (3)	C18–C19	1.532 (4)

Table II. Selected Bond Angles (deg) in 3a

C13–Fe–C12	38.5 (1)	C7–C6–C5	109.1 (2)
C13–Fe–C5	132.8 (1)	C8–C7–C6	115.8 (3)
C13–Fe–C4	170.7 (1)	C9–C8–C7	117.5 (3)
C13–Fe–C3	90.3 (1)	C10–C9–C8	117.7 (3)
C13–Fe–C2	87.8 (1)	C11–C10–C9	115.3 (2)
C13–Fe–C1	98.0 (1)	C10–C11–C4	109.3 (2)
C12–Fe–C5	94.4 (1)	C19–C12–C13	121.4 (2)
C12–Fe–C4	132.6 (1)	C19–C12–Fe	123.8 (2)
C12–Fe–C3	85.6 (1)	C13–C12–Fe	70.5 (1)
C12–Fe–C2	88.7 (1)	C14–C13–C12	120.8 (2)
C12–Fe–C1	136.5 (1)	C14–C13–Fe	123.7 (2)
C5–Fe–C4	38.2 (1)	C12–C13–Fe	71.0 (1)
C5–Fe–C3	88.3 (1)	C15–C14–C13	109.0 (2)
C5–Fe–C2	88.0 (1)	C16–C15–C14	116.0 (3)
C5–Fe–C1	129.1 (1)	C17–C16–C15	118.3 (3)
C4–Fe–C3	91.3 (1)	C18–C17–C16	118.0 (3)
C4–Fe–C2	89.5 (1)	C19–C18–C17	115.1 (2)
C4–Fe–C1	91.0 (1)	C18–C19–C12	109.7 (2)
C3–Fe–C2	172.9 (1)	D1–Fe–D2	132.6 (1)
C3–Fe–C1	93.7 (1)	D1–Fe–C13	151.8 (1)
C2–Fe–C1	93.4 (1)	D1–Fe–C12	113.4 (1)
O1–C1–Fe	177.7 (2)	D1–Fe–C3	89.7 (1)
O2–C2–Fe	178.9 (2)	D1–Fe–C2	88.7 (1)
O3–C3–Fe	178.6 (2)	D1–Fe–C1	110.1 (1)
C11–C4–C5	121.6 (2)	D2–Fe–C5	113.6 (1)
C11–C4–Fe	122.3 (2)	D2–Fe–C4	151.7 (1)
C5–C4–Fe	71.0 (1)	D2–Fe–C3	87.8 (1)
C6–C5–C4	120.3 (2)	D2–Fe–C2	88.1 (1)
C6–C5–Fe	122.9 (2)	D2–Fe–C1	117.3 (1)
C4–C5–Fe	70.8 (1)		

[a] D1 is the midpoint of C4–C5. D2 is the midpoint of C12–C13.

Table III. Equations of Selected Least-Squares Planes in 3a[a]

(a) Plane 1, Defined through atoms
Fe, Cl, Ol, C2, O2, C3, O3
$-0.0232x - 0.6813y + 0.7317z - 5.2957 = 0$
(Fe, −0.019; C1, 0.015; O1, −0.008; C2, −0.04; O2, 0.011; C3, −0.010; O3, 0.015)

(b) Plane 2, defined through Atoms
Fe, Cl, O1, D1, D2
$-0.7257x + 0.5092y + 0.4627z - 2.5024 = 0$
(Fe, −0.004; Cl, −0.005; O1, −0.003; C4, 0.014; C5, −0.013; C12, −0.054; C13 0.056)

Angle between the Two Planes: 89.52°

[a] Deviations (Å) of the atoms from these planes in parentheses.

(12) Cope, A. C.; Ganellin, C. R.; Johnson, H. W.; van Auken, T. V.; Winkler, H. J. S. *J. Am. Chem. Soc.* **1963**, *85*, 3276.
(13) von Büren, M.; Hansen, H.-J. *Helv. Chim. Acta* **1977**, *60*, 2717. von Büren, M. Doctoral Dissertation, Universität Freiburg, Switzerland, 1981.
(14) Grevels, F.-W.; Skibbe, V. *J. Chem. Soc., Chem. Commun.* **1984**, 681.
(15) Skibbe, V. Doctoral Dissertation, Universität Duisburg, 1985.
(16) Quantum yields and mechanistic implications of these processes will be reported in a forthcoming paper.

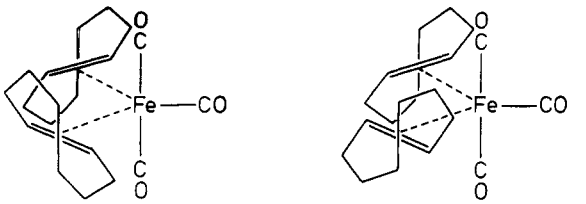

3a (C_2) **3b** (C_S)

$Fe(CO)_4$ complexes,[17] the structure shows a trigonal-bipyramidal arrangement of the ligands around the metal. The C=C double bonds of both cyclooctene rings lie in the equatorial plane together with one carbonyl group, while the other two carbonyl groups occupy the axial positions. A noncrystallographic twofold symmetry axis is passing through the atoms Fe, C1, and O1 which identifies this complex as the C_2 isomer.

The angle C2–Fe–C3 of the two axial CO groups (172.9°) shows a slight deviation from linearity; the trigonal plane (plane 2, Table III) makes an angle of 89.5° with the plane defined by the three carbonyl groups and the iron atom (plane 1). The arrangement of the three ligands in the equatorial plane (Figure 2A) deviates markedly from the ideal trigonal geometry: the angle between the midpoints of the coordinated double bonds enclosing the iron atom is 132.6°, whereas the complementary angles to the equatorial carbonyl group are 110.1° and 117.3°, respectively. The analogous angles of the related complex **1** showed a deviation in the opposite direction which, in that case,[10] was explained in terms of ring tension of the cyclic system attached to the olefinic double bonds. Likewise, the Fe–C(olefin) bond distances of **1** showed a notable difference (0.09 Å) whereas in **3a** the olefinic carbon atoms are nearly equidistant from the iron atom. A lengthening of the double bonds upon coordination (average 1.399 Å; cf. noncomplexed *trans*-cyclooctene derivatives:[18] ca. 1.33–1.34 Å) and an alteration of the bonding angles of the adjacent hydrogen atoms toward 109° reveal some sp^3 character of the involved carbon atoms.[17,19] Both of the two *trans*-cyclooctene rings adopt a crown conformation (Figure 2B) as it has been observed in complexes of *trans*-cyclooctene with copper(I)[20] and platinum(II),[21] respectively, and for a noncomplexed *trans*-cyclooctene derivative[18] as well.

The unit cell contains four **3a** molecules, two of each enantiomer. Intermolecular contacts within the unit cell are observed below 3.0 Å (but above 2.7 Å) just between carbonyl groups and hydrogen atoms.

The presence of both enantiomers in the crystal is in accordance with the observation that the melting point of racemic **3a** (mp 110–112 °C) is higher than that of one pure enantiomer [(−)-**3a**: mp 91–93 °C]; expectedly a ca. 1:1 mixture of **3a**/(−)-**3a** exhibits a further depression, mp 86 °C.

CO Vibrational Force Field Parameters of 3a. In the energy factored force field approximation[22] the three CO stretching vibrations of an $(eq\text{-}L)_2Fe(CO)_3$ complex can be described by four parameters [k(ax), k(eq), i(ax,ax), and

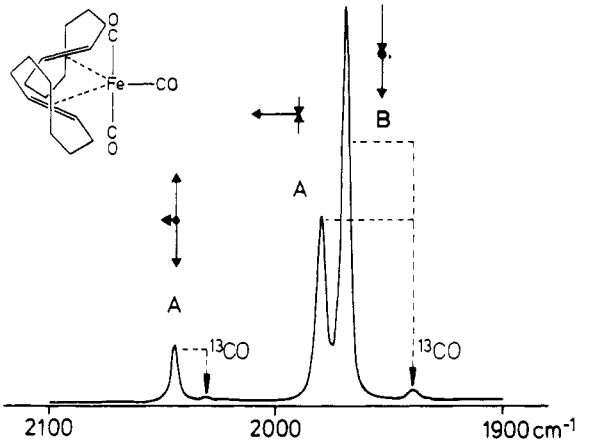

Figure 1. CO stretching vibrational pattern of **3a** in *n*-hexane.

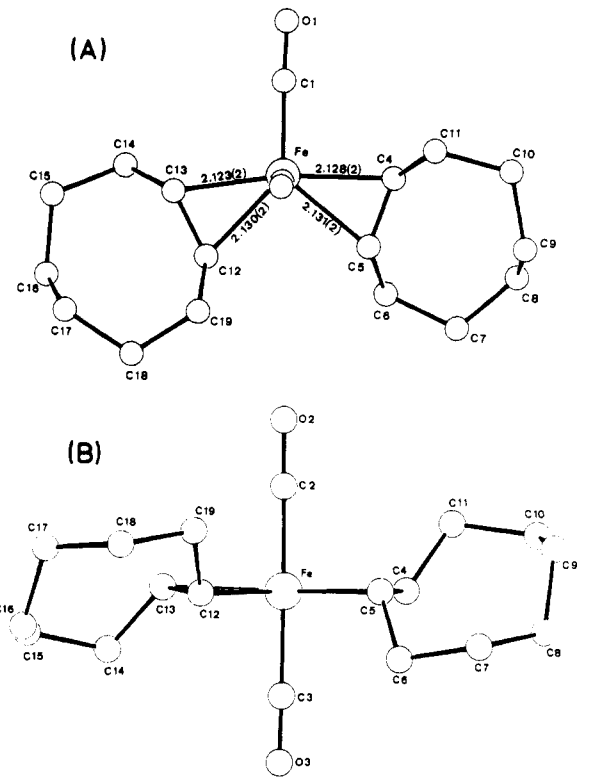

Figure 2. Structure of **3a** in the crystal. (A) View from top of the trigonal bipyramid along O(2)–C(2)–Fe, C(3)–O(3) being hidden underneath Fe. (B) View from the midpoint between C(12)/C(5) to Fe, C(1)–O(1) being hidden behind Fe.

i(ax,eq)]. On the basis of the observed frequencies of the C_2 isomer **3a** [2047.2 (A), 1977.4 (A), and 1970.1 (B) cm^{-1}] and the low-frequency ^{13}CO satellite band at 1940.5 cm^{-1} (Figure 1), the following force field parameters are obtained: k(ax) = 1623.0, k(eq) = 1594.7, i(ax,ax) = 54.9, and i(ax,eq) = 27.3 Nm^{-1}. With use of these values the ν(CO) frequencies of the two isotopomeric ^{13}CO monolabeled species are calculated as follows: **3a′** (ax-^{13}CO) 2033.1 (observed at 2033.2), 1976.7 (hidden underneath the 1977.4 cm^{-1} band of **3a**), and 1940.4 cm^{-1}; **3a″** (eq-^{13}CO) 2043.3 (barely detectable at the low-frequency shoulder of the 2047.2 cm^{-1} band of **3a**), 1970.1 (position identical with the B band of **3a**), and 1937.0 cm^{-1} (nearly coincident with the 1940.5 cm^{-1} band of **3a′**).

The smaller force constants of **3a**, compared with $Fe(CO)_5$ [k(ax) = 1695, k(eq) = 1657 Nm^{-1}][23] and **4** [k(ax)

(17) Krüger, C.; Barnett, B. L.; Brauer, D. in ref 1, p 1.
(18) Ermer, O.; Mason, S. A. *Acta Crystallogr., Sect. B: Struct. Crystallogr. Cryst. Chem.* **1982**, *B38*, 2200 and references cited therein.
(19) Krüger, C. *J. Organomet. Chem.* **1970**, *22*, 697.
(20) Ganis, P.; Lepore, U.; Martuscelli, E. *J. Phys. Chem.* **1970**, *74*, 2439.
(21) Manor, P. C.; Shoemaker, D. P.; Parkes, A. S. *J. Am. Chem. Soc.* **1970**, *92*, 5260.
(22) Braterman, P. S. *Metal Carbonyl Spectra*; Academic: London, 1975.
(23) Bor, G. *Inorg. Chim. Acta* **1969**, *3*, 191.

Table IV. $^{13}C\{^1H\}$ NMR Data of (η^2-*trans*-Cyclooctene)(η^2-olefin)Fe(CO)$_3$ Complexes[a]

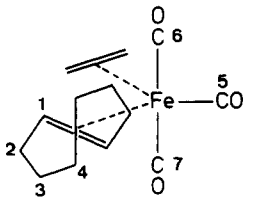

olefin:

3 trans-cyclooctene

5 trans-(=CH–CO_2–CH_2–CH_3)$_2$

6 CH_2=CH–CO_2–CH_3

complex	T, K	δ[b] C(1)	C(2)[c]	C(3)[c]	C(4)[c]	C(5)	C(6) C(7)
3a[d]	193	64.26	42.49	37.85	30.05	218.32	211.50
		63.72	40.96	37.36			
	253	64.0	41.7	37.6	30.1		
		(69.9)	(−7.4)	(−3.3)	(−1.4)		
3b[d]	178	61.87	42.20	37.39	29.97	219.16	210.45/212.68
		60.63	40.46	37.23			
	210	61.4	41.3	37.4	30.0	218.9	210.4/212.5
		(72.5)	(−7.0)	(−3.1)	(−1.3)		
5a[e]	193	73.6	40.2	36.9	29.1	214.9	205.7/204.1
		(60.3)	(−4.2)	(−1.0)	(−0.4)		
6[f]	233	70.3[g]	40.1	36.4	28.6	217.2	208.3/206.0
		(63.6)	(−4.0)	(−0.5)	(0.9)		
		66.2[h]	40.2	36.0		216.3	208.5/207.2
		(67.7)	(−4.2)	(−0.1)			

[a] Note that the numbering scheme differs from those in the X-ray structure analyses of **3a** (Figure 2) and **5a** (Figure 6). [b] In parentheses: $\Delta\delta = \delta$(olefin) − δ(complex). [c] Tentative assignments. [d] In methylcyclohexane-d_{14}, 100.6 MHz. [e] In toluene-d_8, 67.89 MHz, δ(fumarate) C(8) 46.2/44.5 (87.5/89.2), C(9) 175.2/174.7 (−10.6/−10.1), C(10) 60.4/60.1 (0.7/1.0), C(11) 14.7/14.5 (−0.7/−0.5); data for second isomer, **5b**, cf. Experimental Section. [f] In toluene-d_8, 100.6 MHz. [g] Major component, δ(acrylate) C(8), 34.4 (95.9), C(9) 44.6 (84.3), C(10) 175.9 (−9.7), C(11) 50.6 (0.6). [h] Minor component, δ(acrylate) C(8) 37.4 (92.9), C(9) 43.8 (85.1), C(10) 176.5 (−10.3), C(11) 51.1 (0.1).

= 1660, k(eq) = 1623 Nm^{-1}][24], indicate that the olefin is a weaker π-acceptor (and/or stronger σ-donor) than carbon monoxide. At first glance it may be surprising that the introduction of two olefins in the equatorial plane of Fe(CO)$_5$ has a more pronounced effect on the axial CO groups [Δk(ax) = 72 Nm^{-1}] than on the remaining equatorial CO group [Δk(eq) = 62 Nm^{-1}]. However, as the olefins are single-faced π-acceptors with the π^*-orbitals oriented in the equatorial plane, it is only the equatorial CO and not the axial CO groups which is subject to direct competition with the olefins for M → L π-back-donation. In other words, in going from Fe(CO)$_5$ to (η^2-olefin)$_2$Fe(CO)$_3$ the axial CO groups should gain more M → π^*(CO) back-bonding and, consequently, experience a more pronounced reduction of the stretching vibrational force constant than does the equatorial carbon monoxide ligand.

^{13}C NMR Spectra and Dynamic Behavior of 3 in Solution. Carbonyl group site exchange of (η^2-olefin)Fe(CO)$_4$ complexes[25-28] and some (η^2-olefin)Fe(CO)$_{4-n}$L$_n$ derivatives[26] was monitored by variable temperature ^{13}C NMR spectroscopy. The observations have been interpreted in terms of Berry pseudorotation coupled with olefin rotation. The olefin was suggested to take the pivotal position in the square-pyramidal intermediate and to rotate about the fourfold axis (eq 3). The energetic

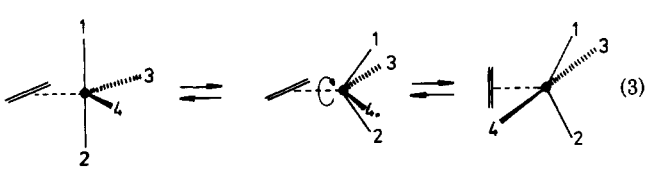

(3)

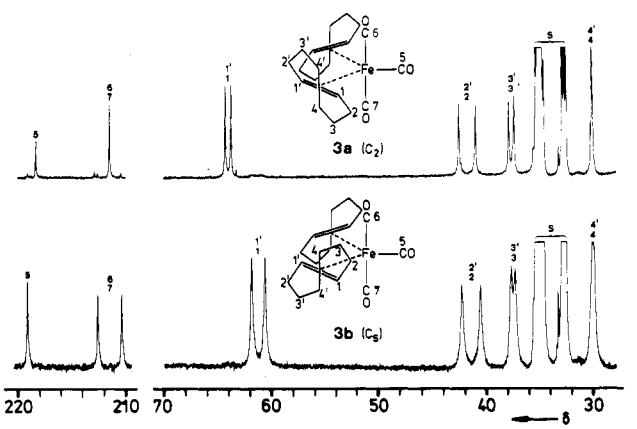

Figure 3. $^{13}C\{^1H\}$ NMR spectra of (η^2-*trans*-cyclooctene)$_2$Fe(CO)$_3$, in methylcyclohexane-d_{14}: **3a** (C_2 isomer) at 193 K; **3b** (C_s isomer) at 178 K.

requirements of this mechanism[29,30] are in accord with the observed activation energies. However, while Berry pseudorotation implies synchronous site exchange of all four carbonyl groups, results obtained with (η^2-methyl acrylate)Fe(CO)$_4$[27] and various (η^2-*cis*-cycloalkene)Fe(CO)$_4$ complexes[31] indicate a sequence of several three-site carbonyl exchange processes to be operative, which involve the two equatorial and one of the axial CO ligands.

In this context the dynamic behavior of (η^2-olefin)$_2$Fe(CO)$_3$ complexes is of particular interest because, in addition to CO scrambling, rotation of the olefin should be directly observable. The $^{13}C\{^1H\}$ NMR spectra of **3a** and **3b** at low temperatures are displayed in Figure 3; the data are summarized in Table IV. In accord with the structure in the crystal (Figure 2) complex **3a** exhibits one set of

(24) Angermund, H. Doctoral Dissertation, Universität Duisburg, 1986.
(25) Kruczynski, L.; LiShingMan, L. K. K.; Takats, J. *J. Am. Chem. Soc.* **1974**, *96*, 4006.
(26) Wilson, S. T.; Coville, N. J.; Shapely, J. R.; Osborn, J. A. *J. Am. Chem. Soc.* **1974**, *96*, 4038.
(27) Faller, J. W. *Adv. Organomet. Chem.* **1977**, *16*, 211.
(28) von Büren, M.; Cosandey, M.; Hansen, H.-J. *Helv. Chim. Acta* **1980**, *63*, 738.
(29) Demuynck, J.; Strich, A.; Veillard, A. *Nouv. J. Chim.* **1977**, *1*, 217.
(30) Albright, T. A.; Hoffmann, R.; Thibeault, J. C.; Thorn, D. L. *J. Am. Chem. Soc.* **1979**, *101*, 3801.
(31) Cosandey, M.; von Büren, M.; Hansen, H.-J. *Helv. Chim. Acta* **1983**, *66*, 1.

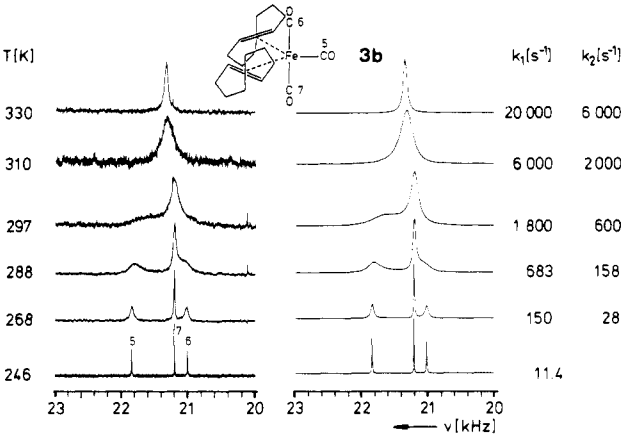

Figure 4. ^{13}C NMR spectrum of **3b** in the carbonyl ligand region, measured (left) at various temperatures and simulated (right) with k_1 (5 ⇌ 6) and k_2 (5/6 ⇌ 7).

Table V. Activation Parameters[a] Obtained from Variable-Temperature $^{13}C\{^1H\}$ NMR Spectra of 3a and 3b

	exchange process	E_a, kcal mol^{-1}	$\Delta H^{\ddagger}$, kcal mol^{-1}	$\Delta S^{\ddagger}$, cal mol^{-1} K^{-1}
3a	olefin rotation			
	C_1, C_1'	9.98 ± 0.3	9.55 ± 0.3	−3.8 ± 2
	C_2, C_2'	9.49 ± 0.3	9.05 ± 0.3	−6.0 ± 2
	average	9.7 ± 0.4	9.3 ± 0.4	−4.9 ± 2
	CO scrambling			
	C_5, C_6 (= C_7)	15.3 ± 0.6	14.8 ± 0.6	6.0 ± 3
3b	olefin rotation			
	C_1, C_1'	8.0 ± 0.5	7.6 ± 0.6	−7.3 ± 3
	C_2, C_2'	8.9 ± 0.3	8.5 ± 0.3	−2.9 ± 2
	average	8.4 ± 0.5	8.0 ± 0.5	−5.1 ± 3
	CO scrambling			
	C_5, C_6	14.4 ± 0.4	13.8 ± 0.4	2.8 ± 1.2
	$C_5/C_6, C_7$	17.4 ± 0.8	16.8 ± 0.8	10.2 ± 3

[a] The error limits stem from regression analyses.

eight signals for the two trans-cyclooctene ligands and two lines with a 1:2 intensity ratio in the carbonyl region. The more intense signal at higher field is assigned to the two equivalent axial CO groups. The position of the equatorial CO signal at lower field is in line with the frequently observed correlation between the CO stretching force constants [3a: k(eq) < k(ax), vide supra] and ^{13}C NMR chemical shifts [cf., e.g., $LM(CO)_5$ complexes: δ(trans-CO) > δ(cis-CO), k(trans-CO) < k(cis-CO)].[32] The *trans*-cyclooctene signal pattern of **3b** is similar to that of **3a**, whereas in the carbonyl region **3b** exhibits three lines of equal intensities in accord with the proposed C_s symmetry.

Raising the temperature results in pairwise equilibration of the *trans*-cyclooctene signals of **3a** and **3b** and, subsequently, in coalescence of the CO resonances. In the case of **3b** the latter process clearly occurs in two steps: at the onset the equatorial and only one of the two axial CO signals start to broaden, and subsequently at higher temperatures the second axial CO group also takes part in the exchange process (Figure 4). This resembles the dynamic behavior of (η^2-*cis*-cycloalkene)$Fe(CO)_4$ complexes[31] where only one of the two axial CO ligands is involved in the initial CO scrambling process. Two sets of activation parameters for the CO site exchange of **3b** (Table V) are obtained from the line-shape analysis of the spectra recorded at various temperatures. For the C_2 isomer **3a**, with two equivalent axial CO groups, the whole process can be described by two equal rate constants. In this case the resulting activation parameters (Table V) are close to the

(32) Buchner, W.; Schenk, W. A. *Inorg. Chem.* **1984**, *23*, 132.

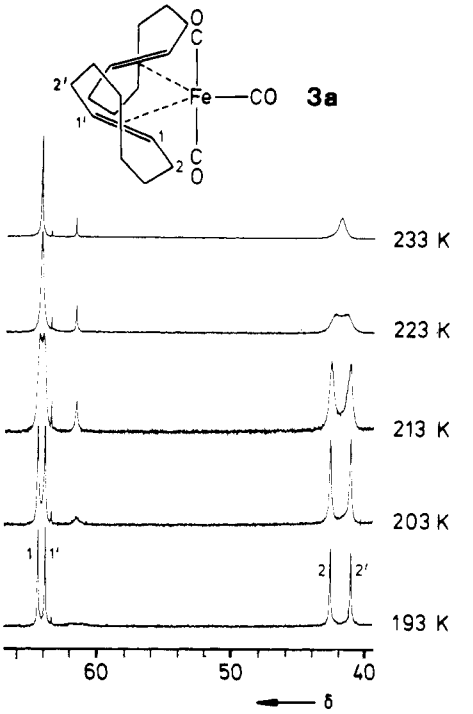

Figure 5. Variable-temperature $^{13}C\{^1H\}$ NMR spectra of **3a** in the hydrocarbon region.

average of the values obtained for **3b**. Noteworthy, CO scrambling in the corresponding (η^2-olefin)$Fe(CO)_4$ complex **4** occurs with a substantially lower energy barrier (E_a = 6 kcal mol^{-1}).[28]

The pairwise equilibration of the *trans*-cyclooctene signals was proven to be an intramolecular process, since it is not affected by the addition of free olefin (racemic *trans*-cyclooctene). Futhermore, intermediate dissociation of metal–olefin bonds should cause, at least to some extent, olefin exchange between different metal centers which implicates isomerization **3a** ⇌ **3b**. However, this was not observed at temperatures up to 40 °C. Thus we assign the observed spectral changes to rotation of the olefin about the metal–olefin bond. Line-shape analyses were performed for the olefinic carbon atoms and for one pair of $-CH_2-$ groups (Figure 5) which gave nearly identical results. For both of the isomers **3a** and **3b**, the barrier for olefin rotation (Table V) is distinctly smaller than the activation energy for CO scrambling, ca. 9 kcal mol^{-1} vs ca. 16 kcal mol^{-1}.

(η^2-Diethyl fumarate)(η^2-*trans*-cyclooctene)$Fe(CO)_3$ (5) and (η^2-Methyl acrylate)(η^3-*trans*-cyclooctene)-$Fe(CO)_3$ (6). In order to gain some more information about the factors that govern the strength of the olefin–iron bond and control the dynamic behavior, we set out for the syntheses of mixed (η^2-olefin)$_2Fe(CO)_3$ complexes, in which direct competition of two different olefins at the same metal center might give rise to mutual influence on their respective σ-donor and/or π-acceptor bonding interactions with the metal.

(η^2-Diethyl fumarate)(η^2-*trans*-cyclooctene)$Fe(CO)_3$ (**5**) represents the first example of this type of complex. It is accessible from either of the two directions illustrated in eq 4, i.e. from the photoreaction of (η^2-*trans*-cyclooctene)$Fe(CO)_4$ (**4**)[28] with diethyl fumarate or from irradiation of (η^2-diethyl fumarate)$Fe(CO)_4$[33] in the presence of *trans*-cyclooctene. The latter procedure yields **3** as a

(33) Schenck, G. O.; Koerner von Gustorf, E.; Jun, M.-J. *Tetrahedron Lett.* **1962**, 1059.

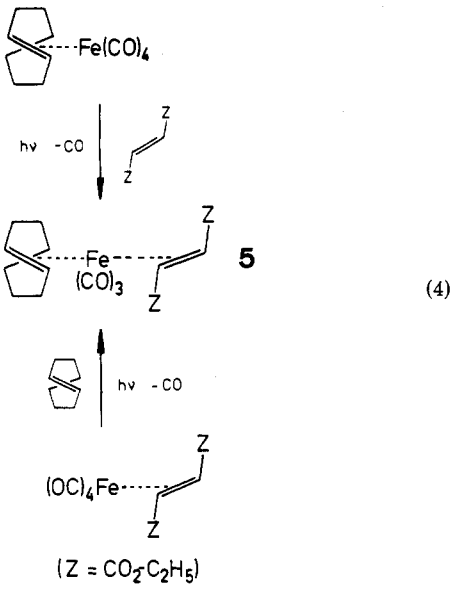

(4)

byproduct resulting from photoinduced olefin exchange upon extended irradiation.

Not unexpectedly, the ^{13}C NMR spectrum of some samples of **5** shows that two isomers, **5a** and **5b**, are present which should be structurally related to the respective isomers of **3**. The main isomer **5a** was isolated in pure state after separation by column chromatography.

Treatment of **5a** with carbon monoxide under pressure at 40 °C in *n*-hexane solution results in quantitative displacement of *trans*-cyclooctene yielding (η^2-diethyl fumarate)Fe(CO)$_4$. Thus it is evident that the fumarate ligand is distinctly stronger bound to the metal than *trans*-cyclooctene. This trend in bond strengths is reflected, too, in the metal–olefin distances determined by an X-ray structure analysis.

The structure of **5a**, displayed in Figure 6 (cf. Tables VI and VII), resembles that of **3a** in a sense that the substituents at the olefin moieties are directed away from each other, thus minimizing steric repulsion. As a notable feature, the metal–carbon bond lengths to the fumarate ligand (Table VI) are significantly shorter, by ca. 0.08 Å, than those to *trans*-cyclooctene. Furthermore, comparing **3a** with **5a** (Figure 7) we note a considerable increase in the *trans*-cyclooctene–iron bond distances; i.e., substitution of one of the cyclooctene ligands in **3a** for a stronger π-acceptor causes substantial weakening of the remaining cyclooctene–metal bond. An analogous trend is observed if **5a** is compared with another fumarate complex, (η^2-diethyl fumarate)(triphenylphosphine)Fe(CO)$_3$:[34] exchange of the phosphine ligand for *trans*-cyclooctene results in a marked lengthening of the Fe–C bond distances to the remaining olefin diethyl fumarate (Figure 7).

The ^{13}C NMR data of **3a** and **5a** (Table IV) correlate well with the bond lengths: the longer the iron–olefin bond distance, the less pronounced is the upfield coordination shift of the olefinic carbon atoms, as it is illustrated by the data displayed in Figure 7.

The barrier for olefin rotation obeys the same order. While coalescence of the olefin carbon atoms of **3a** occurs at ca. −50 °C and E_a for this process is well below 10 kcal mol^{-1}, the fumarate in **5a** does not show line broadening up to the decomposition temperature at ca. +40 °C, and rotation of the *trans*-cyclooctene ligand in this complex is not frozen out down to −80 °C (Figure 8). Noteworthy,

(34) Stainer, M. V. R.; Takats, J. *Inorg. Chem.* **1982**, *21*, 4044. Takats, J., private communication.

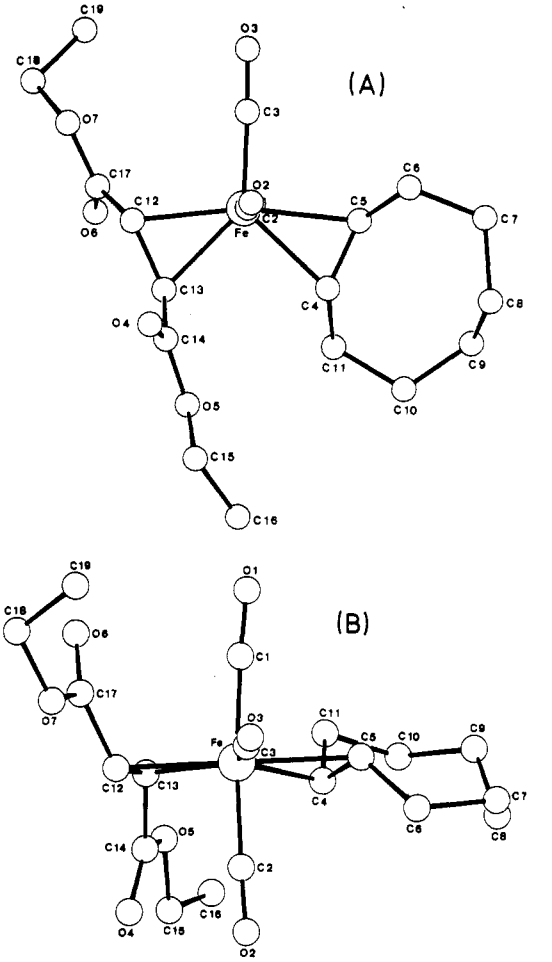

Figure 6. Structure of **5a** in the crystal. (A) View onto the equatorial plane of the trigonal bipyramid along O(2)–C(2)–Fe, C(1)–O(1) being hidden underneath Fe. (B) View along O(3)–C(3)–Fe.

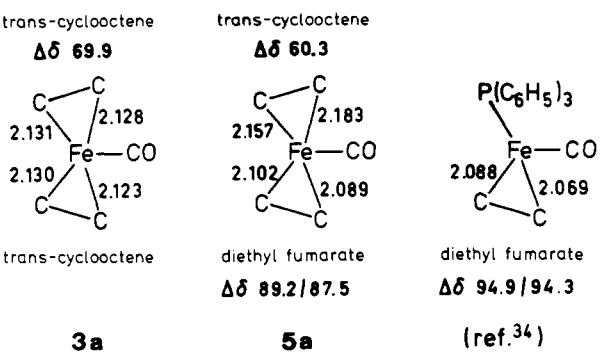

Figure 7. Fe–C(olefin) bond distances (Å) and olefin ^{13}C NMR upfield coordination shifts [$\Delta\delta$ = δ(olefin) − δ(complex)] of **3a**, **5a**, and (η^2-diethyl fumarate)(triphenylphosphine)Fe(CO)$_3$.[34]

Table VI. Selected Bond Distances (Å) in 5a

Fe–C1	1.830 (3)	O7–C18	1.465 (4)
Fe–C2	1.820 (3)	C4–C5	1.393 (4)
Fe–C3	1.797 (3)	C4–C11	1.487 (4)
Fe–C4	2.157 (3)	C5–C6	1.493 (4)
Fe–C5	2.183 (3)	C6–C7	1.537 (6)
Fe–C12	2.089 (3)	C7–C8	1.540 (8)
Fe–C13	2.102 (3)	C8–C9	1.543 (7)
O1–C1	1.134 (3)	C9–C10	1.518 (6)
O2–C2	1.137 (4)	C10–C11	1.552 (5)
O3–C3	1.135 (5)	C12–C13	1.413 (4)
O4–C14	1.203 (4)	C12–C17	1.489 (4)
O5–C14	1.343 (4)	C13–C14	1.472 (4)
O5–C15	1.463 (4)	C15–C16	1.425 (6)
O6–C17	1.202 (4)	C18–C19	1.479 (6)
O7–C17	1.356 (4)		

Table VII. Selected Bond Angles (deg) in 5a

C13–Fe–C12	39.4 (1)	C5–C4–Fe	72.3 (2)
C13–Fe–C5	128.6 (1)	C6–C5–C4	122.3 (3)
C13–Fe–C4	91.8 (1)	C6–C5–Fe	122.3 (2)
C13–Fe–C3	137.1 (1)	C4–C5–Fe	70.3 (2)
C13–Fe–C2	93.4 (1)	C7–C6–C5	108.8 (3)
C13–Fe–C1	90.5 (1)	C8–C7–C6	115.5 (3)
C12–Fe–C5	167.9 (1)	C9–C8–C7	119.1 (4)
C12–Fe–C4	130.9 (1)	C10–C9–C8	118.5 (3)
C12–Fe–C3	97.9 (1)	C11–C10–C9	115.2 (3)
C12–Fe–C2	90.4 (1)	C10–C11–C4	108.5 (3)
C12–Fe–C1	94.1 (1)	C17–C12–C13	119.7 (2)
C5–Fe–C4	37.4 (1)	C17–C12–Fe	111.4 (2)
C5–Fe–C3	94.1 (1)	C13–C12–Fe	70.8 (2)
C5–Fe–C2	91.5 (1)	C14–C13–C12	120.1 (2)
C5–Fe–C1	84.2 (1)	C14–C13–Fe	113.8 (2)
C4–Fe–C3	131.1 (1)	C12–C13–Fe	69.8 (2)
C4–Fe–C2	86.9 (1)	C13–C14–O5	110.3 (2)
C4–Fe–C1	90.6 (1)	C3–Fe–C2	88.9 (1)
C13–C14–O4	126.6 (3)	C3–Fe–C1	89.9 (1)
O5–C14O4	123.1 (3)	C2–Fe–C1	175.5 (1)
C16–C15–O5	108.7 (3)	C15–O5–C14	116.0 (3)
C12–C17–O7	110.7 (2)	C18–O7–C17	117.4 (3)
C12–C17–O6	125.7 (3)	O1–C1–Fe	174.7 (2)
O7–C17–O6	123.6 (3)	O2–C2–Fe	175.5 (3)
C19–C18–O7	110.5 (3)	O3–C3–Fe	177.4 (3)
C11–C4–Fe	122.4 (2)	C11–C4–C5	121.4 (3)

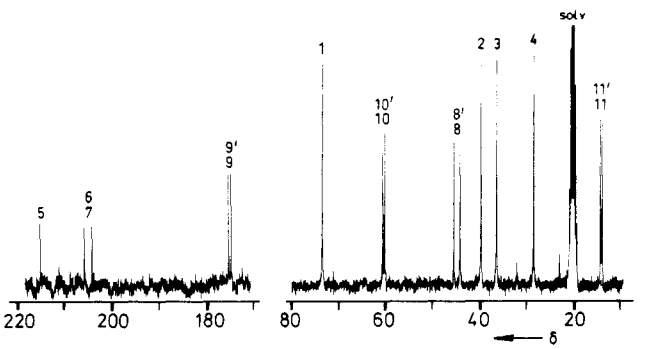

Figure 8. $^{13}C\{^1H\}$ NMR spectrum of (η^2-*trans*-cyclooctene)(η^2-diethyl fumarate)Fe(CO)$_3$ (**5a**) in toluene-d_8 at 193 K (numbering scheme, cf. Table IV).

inspection of the line shape of the ^{13}CO signals indicates that complex **5a** does not undergo CO scrambling up to the highest temperature reached in the NMR measurements, +40 °C.

The mixed acrylate/*trans*-cyclooctene complex **6** is prepared by olefin exchange of the labile (η^2-methyl acrylate)$_2$Fe(CO)$_3$[8] with *trans*-cyclooctene (eq 5). **6** is less

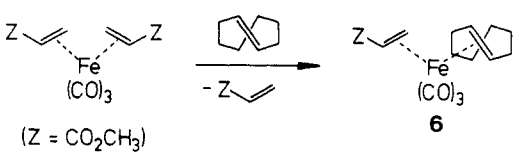

(Z = CO_2CH_3) **6** (5)

stable than **3a/b** and **5a**. It takes up carbon monoxide already at room temperature. However, in this case it is not *trans*-cyclooctene but the α,β-unsaturated ester which is displaced from the metal, yielding (η^2-*trans*-cyclooctene)Fe(CO)$_4$.

With respect to the dynamic behavior, **6** represents a more complicated situation than **3** and **5**. A total number of four isomers (together with the respective enantiomers) is possible. Rotation of the acrylate ligand by 180° is not a degenerate process but results in pairwise interconversion of the isomers of **6**. One of the two pairs is present in the pure material isolated after column chromatography. At −40 °C the $^{13}C\{^1H\}$ NMR spectrum exhibits two sets of signals with different intensities (Figure 9, Table IV). Again, as observed in the case of **5a**, rotation of *trans*-

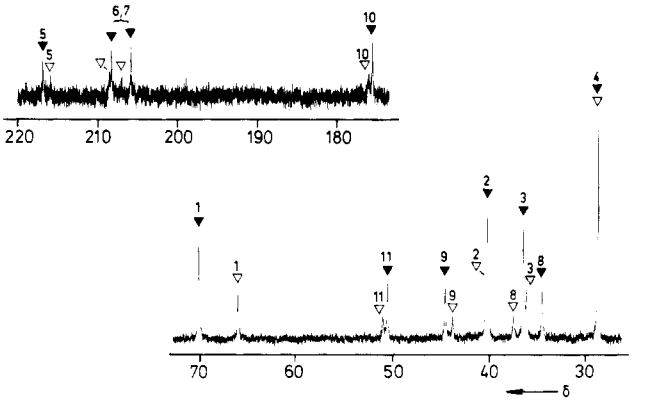

Figure 9. $^{13}C\{^1H\}$ NMR spectrum of (η^2-*trans*-cyclooctene)(η^2-methyl acrylate)Fe(CO)$_3$ (**6**) (▼, major isomer; ▽, minor isomer), in toluene-d_8 at 233 K (numbering scheme, cf. Table IV).

cyclooctene about the metal–olefin bond axis is not frozen out down to −80 °C; however, at this temperature we note the onset of broadening of the cyclooctene signals. On the other hand, raising the temperature to +20 °C results in pairwise coalescence and gradual resharpening of the signals of the two isomers in the region of the organic ligands. Merely the CO lines have not reappeared at this temperature.

Discussion

The exceptional coordination properties of *trans*-cyclooctene are in striking contrast to those of *cis*-cyclooctene which forms an extremely labile (η^2-olefin)$_2$Fe(CO)$_3$ complex.[4] This can be understood on the basis of its π- and π^*-orbital energies[35–37] which would predict *trans*-cyclooctene to be a better donor and a better π-acceptor than the cis isomer: ring strain in the eight-membered trans-cycloalkene causes twisting about the C=C double bond, thus lowering the olefin π^*-orbital energy and increasing the olefin π-orbital energy, compared with the *cis*-cycloalkene. Upon coordination to the metal the C—C=C—C conformational angle decreases from 136° in free *trans*-cyclooctene[18] to ca. 125° in **3a** and **5a**. This way the donor and π-acceptor capacities of *trans*-cyclooctene are further improved, thus directly strengthening the metal–olefin interaction, and in addition the eight-membered ring gains some stabilization owing to relief from ring strain.

Replacement of one *trans*-cyclooctene ligand by a stronger π-accepting olefin will diminish π-back-donation to the remaining ligands. This becomes apparent in the series **3a/3b**, **6**, and **5a**. Variable-temperature NMR spectra reveal a decrease in the barrier of rotation about the axis of the remaining (*trans*-cyclooctene)–iron bond, which is indicative of weaker metal→π^*(*trans*-cyclooctene) back-bonding. Furthermore, we note a gradual upfield shift of the carbonyl ^{13}C NMR resonances (Table IV) which may be interpreted in terms of a lower degree of metal→π^*(CO) back-donation,[38–40] although the intrinsic origin of such effects has been discussed controversely.

Regarding the relative importance of the π(olefin)→metal and metal→π^*(olefin) interactions, it seems that the latter component of the iron–(*trans*-cyclooctene) bond

(35) Allan, M.; Haselbach, E.; von Büren, M.; Hansen, H.-J. *Helv. Chim. Acta* **1982**, *65*, 2133.
(36) Batich, C.; Ermer, O.; Heilbronner, E.; Wiseman, J. R. *Angew. Chem.* **1973**, *85*, 302; *Angew. Chem., Int. Ed. Engl.* **1973**, *12*, 312.
(37) Bischof, P.; Heilbronner, E. *Helv. Chim. Acta* **1970**, *53*, 1677.
(38) Braterman, P. S.; Milne, D. W.; Randall, E. W., Rosenberg, E. *J. Chem. Soc., Dalton Trans.* **1973**, 1027.
(39) Bodner, G. M.; Todd, L. J. *Inorg. Chem.* **1974**, *13*, 1335.
(40) Gansow, O. A.; Schexnayder, D. A.; Kimura, B. Y. *J. Am. Chem. Soc.* **1972**, *94*, 3406.

plays the major role in the above compounds. Clearly, if π(olefin)→metal donation would be predominant, as it has been suggested for (η^2-*trans*-cyclooctene)Fe(CO)$_4$,[13,28,35] one should expect that the introduction of a better acceptor such as fumarate (**3** → **5**) results in strengthening of the remaining *trans*-cyclooctene–iron bond, contrary to the experimental findings.

However, one has to be cautious in generalizing this conclusion. If in any case the π-acceptor ability of the olefin would determine the olefin–iron bond strength, olefins such as acrylate or fumarate should form the most stable (η^2-olefin)$_2$Fe(CO)$_3$ complexes. On the contrary, (η^2-methyl acrylate)$_2$Fe(CO)$_3$ is a rather labile compound,[8] and various attempts to synthesize (η^2-diethyl fumarate)$_2$Fe(CO)$_3$ analogous to eq 1 and 2 failed. Obviously the Fe(CO)$_3$ moiety is limited in its capability to meet the demand of olefin ligands for d(π) electron density, and thus the overall stability of (η^2-olefin)$_2$Fe(CO)$_3$ systems is the result of a delicate balance between the donor and acceptor properties of both of the two olefins.

Although C–C bond formation between the two olefins was not a particular intent of the present study, it is of interest to note that in no case oxidative cyclization of a (η^2-olefin)$_2$Fe(CO)$_3$ complex with formation of a ferracyclopentane derivative (or a related CO insertion product) was observed (cf. ref 4). In this context we wish to emphasize that the previously reported formation of a tetracarbonylferracyclopentane complex via (η^2-methyl acrylate)$_2$Fe(CO)$_3$[8] does not proceed straightforwardly by oxidative cyclization of the (η^2-olefin)$_2$Fe(CO)$_3$ complex (cf. the theoretical study on this problem by Hoffman et al.[7]) but most probably involves an intermediate dicarbonylorganoiron species.[41]

With regard to the dynamic behavior of trigonal-bipyramidal bis(η^2-olefin)tricarbonyliron complexes the results presented in this paper reveal that olefin rotation in compounds **3** and **6** (and, at least, *trans*-cyclooctene rotation in **5a**) is independent from CO scrambling and occurs with a substantially lower activation energy. This is in striking contrast to the behavior of (η^2-olefin)Fe(CO)$_4$ compounds, particularly those with a *cis*-cycloalkene as the olefin ligand,[31] which clearly demonstrates that in those compounds olefin rotation is slower than CO site exchange. Calculations on (η^2-ethene)Fe(CO)$_4$ indicate an energy difference of 31 kcal mol^{-1} between the orientation of the C=C unit in the equatorial plane and the upright position.[29] In view of such a high value it seems unlikely that the trigonal-bipyramidal geometry of (η^2-olefin)$_2$Fe(CO)$_3$ complexes is maintained during the olefin rotation, which is associated with an activation energy as low as ca. 9 kcal mol^{-1} in case of **3**. One could assume, therefore, that this process takes place with concomitant distortion of the complex toward, e.g., square-pyramidal geometry, eq 6 and 7, using either an olefin or a CO group as the pivotal ligand (a_1, a_2, and e are axial and equatorial CO ligands, respectively).

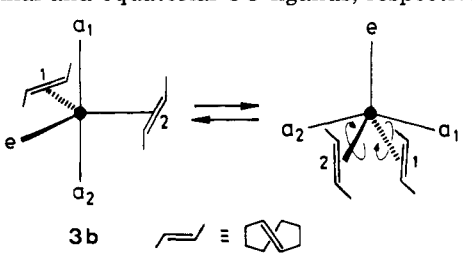

(6)

The discussion on the mechanism of carbonyl scrambling still remains somewhat speculative, notwithstanding the

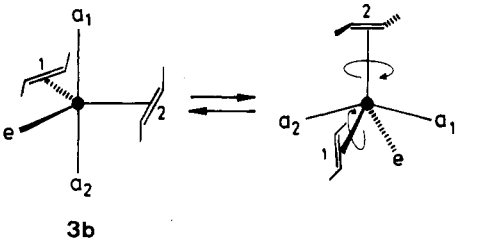

(7)

amount of information on such processes in (η^2-olefin)-carbonyliron systems which has now been accumulated and which allows us to eliminate some of the possible intramolecular motions describing positional exchange in trigonal-bipyramidal molecules.[42] There are some observations which indicate that CO scrambling in (η^2-olefin)$_2$Fe(CO)$_3$ complexes is associated with rotation of the olefinic ligands, either as a prerequisite or as an immanent consequence, thus ruling out a simple ax-CO/eq-CO site exchange: (a) with complex **1**, in which the two olefinic moieties are held in a fixed orientation relative to each other, CO scrambling is not observed[10] up to the onset of decomposition at ca. +80 °C; (b) comparison of **6** and **3a**/**3b** shows that the introduction of a stronger π-accepting olefin (with a higher rotational barrier) impedes CO scrambling, by analogy with previous reports on (η^2-olefin)Fe(CO)$_4$ complexes;[26] (c) the behavior of **5a** indicates that CO scrambling does not occur if only one of the two olefins rotates.

Clearly, the reversible processes depicted in eq 6 and 7 as such do not result in CO scrambling. However, square-pyramidal geometries of this kind may be involved in sequential Berry pseudorotational rearrangements. The mechanism shown in eq 8 includes three Berry pseudo-

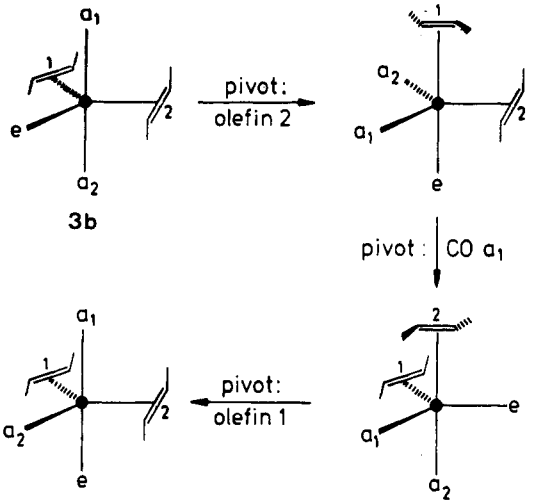

(8)

rotational steps using an olefin, a CO group, and the respective other olefin as the pivotal ligand. This pathway would account for the higher activation energy of CO scrambling compared with olefin rotation because the axial position of an olefin in the trigonal-bipyramidal intermediate geometry is energetically less favorable[29] than the basal or apical positions in the square pyramids involved in eq 6 and 7. Furthermore, in steps 1 and 3 of eq 8 the respective pivotal olefin has to rotate by 90° (cf. eq 3), thus accounting for the fact that CO scrambling depends on the rotational barriers (i.e., on the π-acceptor abilities) of both of the two olefins. Discrimination between the nonequivalent CO groups a_1 and a_2 (which accounts for the

(41) Grevels, F.-W. Habilitationsschrift, Universität Duisburg, 1981.

(42) Ugi, I.; Marquarding, D.; Klusacek, H.; Gillespie, P.; Ramirez, F. *Acc. Chem. Res.* **1971**, *4*, 288.

stepwise CO scrambling observed in case of the C_s isomer **3b**, Figure 4) occurs in step 2, in which one of them is chosen as the pivotal ligand. The final result is a_2/e or a_1/e two-site exchange, depending on whether a_1 or a_2 serves as the pivotal ligand in step 2. It should be noted that a_1 and a_2 take their respective positions, regardless whether olefin 1 or olefin 2 acts as the pivot in steps 1 and 2, respectively. By contrast, in case of the C_2 isomer **3a** each of the two axial CO groups has an equal chance to undergo site exchange with the equatorial CO group.

Alternatively, the non-Berry CO scrambling mechanism suggested for (η^2-*cis*-cycloalkene)$Fe(CO)_4$ complexes[31] could be adapted to the (η^2-olefin)$_2Fe(CO)_3$ system (eq 9).

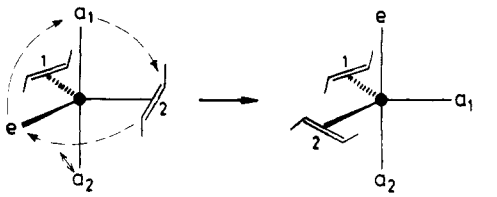

3b (9)

It involves rotation of a group of three ligands (e.g., CO a_1, olefin 2, CO e) relative to the other two in a distorted trigonal-bipyramidal geometry and would account for the stepwise occurrence of CO scrambling, i.e., for the discrimination between the two nonequivalent axial CO groups. However, it does not readily rationalize the association of CO scrambling with olefin rotation.

Experimental Section

All reactions and manipulations were carried out under argon and in argon-saturated solvents. The following materials were prepared according to literature procedures: *trans*-cyclooctene[43] (modified procedure on larger scale), (−)-*trans*-cyclooctene,[12] (η^2-*trans*-cyclooctene)$Fe(CO)_4$,[13] (η^2-diethyl fumarate)$Fe(CO)_4$ (analogous to the dimethyl ester complex),[44] (η^2-methyl acrylate)$_2Fe(CO)_3$,[8] and (η^2-*cis*-cyclooctene)$_2Fe(CO)_3$.[4] Analytical grade solvents (Merck) were used as received. Melting points were determined on a Reichert-Kofler apparatus. Microanalyses were performed by Dornis and Kolbe, Mülheim a.d. Ruhr. Spectra were recorded by using the following instruments: NMR, Bruker AM 400 and AM 100; IR, Perkin-Elmer 580 in combination with Data Station 3600; UV–vis, Perkin-Elmer 320 and Cary 219.

(η^2-*trans*-Cyclooctene)$_2Fe(CO)_3$ (3). A cold mixture of (η^2-*cis*-cyclooctene)$_2Fe(CO)_3$ (**2**) (3.60 g, 10 mmol), *trans*-cyclooctene (2.32 g, 21 mmol), and diethyl ether (20 mL) is stirred and allowed to warm from −78 °C to ambient temperature. Subsequent cooling to −30 °C precipitates pure **3a** which is separated by inverse filtration and dried under vacuum: yellow crystals; mp 110–112 °C (1.13 g, 31.4%). Cooling the filtrate to −78 °C yields a second crop of crystals (1.51 g, 41.9%; ^{13}C NMR **3a**/**3b** = ca. 20/80), and evaporation to dryness of the mother liquor yields a third fraction (0.68 g, 18.9%; ^{13}C NMR **3a**/**3b** = ca. 50/50). Crystals of **3a** suitable for X-ray crystallography were obtained by recrystallization from *n*-heptane. Repetitive recrystallization of the **3a**/**3b** mixtures from hexane and/or diethyl ether yields pure **3b** [yellow crystals; mp 95–96 °C; $\bar{\nu}$(CO) 2046 (w), 1981.5 (m), 1971 (st) cm^{-1}] in addition to further amounts of **3a**. Anal. Calcd for $C_{19}H_{28}FeO_3$: C, 63.34; H, 7.83; Fe, 15.50; mol wt, 360.3. Found (**3a**/**3b** mixture) C, 63.46; H, 7.51; Fe, 15.48; mol wt, 364 (cryoscopic benzene).

(−)-[η^2-(−)-*trans*-Cyclooctene]$_2Fe(CO)_3$ [(−)-3a]. (η^2-*cis*-Cyclooctene)$_2Fe(CO)_3$ (**2**) (0.83 g, 2.3 mmol) is dissolved at −40 °C in a solution of (−)-*trans*-cyclooctene (0.67 g, 6.1 mmol; prepared from (+)-[η^2-(−)-*trans*-cyclooctene][(+)-α-methylbenzylamine]$PtCl_2$[12]) in *n*-heptane (200 mL). The solution is stirred and allowed to warm to ambient temperature. After evaporation in vacuo to dryness the crude product (0.80 g) is recrystallized from *n*-hexane/methanol (1:2, v/v). (−)-**3a**: 0.58 g (70%) of yellow crystals; mp 91–93 °C; IR [$\bar{\nu}$(CO)] and $^{13}C\{^1H\}$ NMR data are identical with those of **3a**; CD (in *n*-hexane) λ/nm (θ/deg 100 mL dm^{-1} mol^{-1}) 430 (0), 347 (−4700), 340 (0), 265 (14 200, sh), 240 (30 000), 225 (19 500, sh), 213 (0); $[\alpha]^{23}_{436}$ −130°, $[\alpha]^{23}_{546}$ −7.8°, $[\alpha]^{23}_{578}$ −2°, $[\alpha]^{23}_{D}$ −1.5° (in *n*-heptane). The crude product (−)-**3a** was free from **3b**, as proven by ^{13}C NMR spectroscopy, when a sample of (+)-[η^2-(−)-*trans*-cyclooctene][(+)-α-methylbenzylamine]$PtCl_2$ with $[\alpha]^{27}_{D}$ 71.4° was used to generate (−)-*trans*-cyclooctene. Starting with another sample of the platinum complex, with $[\alpha]^{27}_{D}$ 65.6°, the resulting (−)-**3a** product contained ca. 5–8% **3b**.

Table VIII. Crystallographic Data of 3a and 5a and Details of Data Collection

	3a	5a
chemical formula	$C_{19}H_{28}FeO_3$	$C_{19}H_{26}FeO_7$
mol wt	360.3	422.3
color of crystal	yellow	yellow
cryst system	monoclinic	orthorhombic
space group	$P2_1/n$ (No. 14)	$P2_12_12_1$ (No. 19)
unit cell parameters:		
reflections used	74 ($10.5 \le \theta \le 23.2$)	72 ($12.9 \le \theta \le 23.2$)
a, Å	12.069 (2)	7.811 (1)
b, Å	8.278 (1)	13.167 (1)
c, Å	18.815 (2)	20.432 (2)
β, deg	98.386 (9)	
V, Å^3	1859.7	2101.2
Z	4	4
d_{calcd}, g cm^{-3}	1.29	1.33
μ(Mo Kα), cm^{-1}	8.20	7.48
λ, Å	0.710 69	0.710 69
data collectn limits, deg	$1.1 \le \theta \le 27.4$	$1.0 \le \theta \le 28.9$
total no. of reflctns	6300 ($\pm h,\pm k,+l$)	5955 ($\pm h,\pm k,+l$)
no. of independent reflctns[a]	4218 ($2/m$)	5506 (222)
no. of obsd reflectns	2902 [$I \ge 2\sigma(I)$]	4158 [$I \ge 2\sigma(I)$]
no. of refined parameters	320	244
$(\sin\theta)/\lambda_{max}$	0.65	0.679
$F(000)$	768	888
error of fit	1.73	2.13
R	0.034	0.037
R_w	0.037	0.045
final diff Fourier, e Å^{-3}	0.58	0.48

[a] After averaging according to point symmetry: $2/m$ for **3a** and 222 for **5a**.

(η^2-*trans*-Cyclooctene)(η^2-diethyl fumarate)$Fe(CO)_3$ (5). (a) Diethyl fumarate (3.72 g, 21.6 mmol) and complex **4** (3.0 g, 10.8 mmol) in *n*-hexane (500 mL) are irradiated in an immersion lamp apparatus (solidex glass, Philips HPK 125-W mercury lamp) for 6 h. After evaporation of the solvent the crude product is purified by column chromatography on silica using first *n*-hexane and then *n*-hexane/diethyl ether (9/1) eluents. The first fractions, containing unreacted **4** and small amounts of other products, are discarded. The product **5** is eluted in the last fraction which yields, after recrystallization from *n*-hexane, 1.82 g of yellow crystals of **5a** (39.9%); mp 69 °C; IR $\bar{\nu}$(CO) 2081.5 (w), 2019 (st), 2021 (sh), 2005.5 (m), 1707.5 (w, ester CO) cm^{-1} (in *n*-hexane). Anal. Calcd for $C_{19}H_{26}FeO_7$: C, 54.04; H, 6.21; Fe, 13.26. Found: C, 54.06; H, 6.25; Fe, 13.38. Crystals of **5a** suitable for X-ray crystallography were obtained by recrystallization from *n*-hexane.

(b) *trans*-Cyclooctene (0.57 g, 5.2 mmol) and (η^2-diethyl fumarate)$Fe(CO)_4$ (1.38 g, 4.1 mmol) in *n*-hexane (250 mL) are irradiated, as described above, for 20 min. Workup and recrystallization, as described above, yields **5** as a yellow amorphous material, 0.71 g (41%), identified by IR and ^{13}C NMR spectroscopy. In addition to the resonances of **5a** (cf. Table IV) the ^{13}C NMR spectrum shows a second set of signals with ca. 30% intensity which are assigned to a second isomer, **5b**: δ 70.9, 39.1,

(43) Vedejs, E.; Snoble, K. A. J.; Fuchs, P. L. *J. Org. Chem.* **1973**, *38*, 1178.
(44) Weiss, E.; Stark, K.; Lancaster, J. E.; Murdoch, H. D. *Helv. Chim. Acta* **1963**, *46*, 288.

Table IX. Atomic Fractional Coordinates with Standard Deviations in Parentheses for 3a

atom	x	y	z
Fe	0.1994 (1)	0.1099 (1)	0.4510 (1)
O1	0.0303 (2)	−0.0754 (3)	0.3566 (1)
O2	0.0325 (2)	0.3036 (3)	0.5136 (1)
O3	0.3890 (2)	−0.0631 (2)	0.4041 (1)
C1	0.0954 (2)	−0.0052 (3)	0.3944 (1)
C2	0.0963 (2)	0.2282 (3)	0.4888 (1)
C3	0.3148 (2)	0.0041 (3)	0.4214 (1)
C4	0.2011 (2)	0.2869 (3)	0.3692 (1)
C5	0.2780 (2)	0.3308 (3)	0.4286 (1)
C6	0.4009 (2)	0.3428 (4)	0.4224 (2)
C7	0.4250 (3)	0.5100 (4)	0.3929 (2)
C8	0.3536 (3)	0.5576 (4)	0.3220 (2)
C9	0.2354 (3)	0.6256 (4)	0.3257 (2)
C10	0.1348 (3)	0.5229 (4)	0.2937 (2)
C11	0.1008 (2)	0.3901 (4)	0.3431 (2)
C12	0.2909 (2)	0.0865 (3)	0.5561 (1)
C13	0.2122 (2)	−0.0388 (3)	0.5437 (1)
C14	0.2491 (2)	−0.2125 (3)	0.5451 (1)
C15	0.2639 (3)	−0.2737 (4)	0.6229 (2)
C16	0.3453 (3)	−0.1783 (4)	0.6768 (2)
C17	0.3027 (3)	−0.0224 (4)	0.7090 (2)
C18	0.3474 (3)	0.1399 (4)	0.6858 (1)
C19	0.2866 (2)	0.2074 (3)	0.6149 (1)
H4	0.231 (2)	0.240 (3)	0.330 (1)
H5	0.256 (2)	0.410 (3)	0.461 (1)
H6a	0.422 (2)	0.258 (3)	0.391 (1)
H6b	0.445 (2)	0.325 (3)	0.470 (1)
H7a	0.500 (3)	0.506 (4)	0.394 (2)
H7b	0.415 (2)	0.592 (3)	0.431 (1)
H8a	0.350 (2)	0.468 (3)	0.289 (1)
H8b	0.393 (2)	0.643 (3)	0.303 (1)
H9a	0.231 (2)	0.649 (3)	0.374 (1)
H9b	0.232 (2)	0.731 (3)	0.300 (1)
H10a	0.075 (2)	0.589 (3)	0.278 (2)
H10b	0.150 (2)	0.473 (3)	0.249 (1)
H11a	0.044 (2)	0.326 (3)	0.315 (1)
H11b	0.074 (2)	0.446 (3)	0.385 (1)
H12	0.364 (2)	0.062 (3)	0.548 (1)
H13	0.144 (2)	−0.024 (3)	0.566 (1)
H14a	0.200 (2)	−0.274 (3)	0.516 (1)
H14b	0.319 (2)	−0.221 (3)	0.525 (1)
H15a	0.286 (2)	−0.379 (3)	0.622 (1)
H15b	0.190 (2)	−0.276 (3)	0.641 (1)
H16a	0.410 (2)	−0.156 (3)	0.656 (1)
H16b	0.372 (2)	−0.247 (3)	0.716 (1)
H17a	0.320 (2)	−0.032 (3)	0.758 (1)
H17b	0.222 (2)	−0.025 (3)	0.701 (1)
H18a	0.342 (2)	0.219 (3)	0.724 (1)
H18b	0.430 (2)	0.131 (3)	0.682 (1)
H19a	0.213 (2)	0.233 (3)	0.620 (1)
H19b	0.318 (2)	0.308 (3)	0.604 (1)

Table X. Atomic Fractional Coordinates with Standard Deviations in Parentheses for 5a

atom	x	y	z
Fe	0.1004 (1)	−0.0079 (1)	0.1607 (1)
O1	0.4206 (3)	0.0386 (2)	0.0895 (1)
O2	−0.1923 (3)	−0.0517 (2)	0.2477 (1)
O3	0.1408 (4)	0.1817 (2)	0.2344 (2)
O4	−0.2905 (3)	−0.1227 (2)	0.1128 (1)
O5	−0.1035 (3)	−0.2211 (1)	0.0592 (1)
O6	0.1238 (3)	0.1191 (2)	0.0078 (1)
O7	−0.0390 (3)	0.2233 (2)	0.0690 (1)
C1	0.2950 (4)	0.0194 (2)	0.1141 (1)
C2	−0.0821 (4)	−0.0375 (2)	0.2126 (2)
C3	0.1294 (4)	0.1078 (3)	0.2062 (2)
C4	0.1886 (4)	−0.1604 (2)	0.1796 (2)
C5	0.2717 (4)	−0.0958 (3)	0.2231 (1)
C6	0.2468 (5)	−0.1030 (4)	0.2955 (2)
C7	0.3675 (5)	−0.1861 (5)	0.3223 (2)
C8	0.3522 (5)	−0.2907 (4)	0.2893 (3)
C9	0.4473 (5)	−0.3098 (3)	0.2246 (3)
C10	0.3434 (5)	−0.3213 (3)	0.1621 (2)
C11	0.2854 (4)	−0.2203 (2)	0.1301 (2)
C12	−0.0634 (4)	0.0490 (2)	0.0888 (1)
C13	−0.0255 (4)	−0.0535 (2)	0.0748 (2)
C14	−0.1558 (4)	−0.1328 (2)	0.0852 (2)
C15	−0.2169 (5)	−0.3080 (3)	0.0691 (2)
C16	−0.1227 (7)	−0.3989 (3)	0.0565 (2)
C17	0.0197 (4)	0.1310 (2)	0.0502 (2)
C18	0.0351 (5)	0.3127 (3)	0.0368 (2)
C19	0.1848 (7)	0.3499 (3)	0.0736 (2)
H4	0.1176	−0.2004	0.1986
H5	0.3960	−0.0789	0.2093
H6a	0.1354	−0.1182	0.3022
H6b	0.2377	−0.0405	0.3212
H7a	0.3328	−0.1928	0.3714
H7b	0.5001	−0.1619	0.3160
H8a	0.2301	−0.3058	0.2807
H8b	0.3986	−0.3436	0.3212
H9a	0.5411	−0.2620	0.2230
H9b	0.5161	−0.3627	0.2346
H10a	0.2461	−0.3652	0.1791
H10b	0.3604	−0.3779	0.1185
H11a	0.3914	−0.1781	0.1180
H11b	0.1973	−0.2571	0.0946
H12	−0.1771	0.0553	0.1070
H13	0.0768	−0.0747	0.0383
H15a	−0.3124	−0.2867	0.0402
H15b	−0.2892	−0.3044	0.1168
H16a	−0.0758	−0.3994	0.0106
H16b	−0.0160	−0.4033	0.0872
H16c	−0.1898	−0.4621	0.0640
H18a	−0.0740	0.3490	0.0247
H18b	0.0724	0.2927	−0.0186
H19a	0.2787	0.2725	0.0764
H19b	0.1579	0.3526	0.1164
H19c	0.2007	0.4164	0.0386

36.4, 28.8 (*trans*-cyclooctene); 44.9/43.9 (diethyl fumarate, other signals coincident with those of **5a**); 215.2, 206.3, 204.0 (CO).

(η^2-*trans*-Cyclooctene)(η^2-methyl acrylate)Fe(CO)$_3$ (6). A solution of *trans*-cyclooctene (0.50 g, 4.4 mmol) and methyl acrylate (0.14 g, 1.6 mmol) in *n*-hexane (65 mL) is cooled to −30 °C, added to (η^2-methyl acrylate)$_2$Fe(CO)$_3$ (1.31 g, 4.2 mmol), and allowed to warm to ambient temperature. After 15 min the solvent is removed under vacuum. (η^2-Methyl acrylate)Fe(CO)$_4$, formed by partial decomposition, is sublimed at 20 °C (10^{-2} Torr). The residual crude product is purified by column chromatography at 0 °C on silica, using first *n*-hexane and then *n*-hexane/diethyl ether (9/1) eluents. The first fractions are discarded; the product **6** is eluted in the last fraction and recrystallized from *n*-hexane (containing 5% methyl acrylate) to yield **6** as a yellow solid: 0.71 g (50%); mp 57 °C; IR $\bar{\nu}$(CO) 2071 (w), 2064 (vw), 2008.5 (st), 1990.5 (st), 1715 (w, ester CO) cm^{-1} (in *n*-hexane). Anal. Calcd for $C_{15}H_{20}FeO_5$: C, 53.60; H, 6.00; Fe, 16.61. Found: C, 53.14; H, 5.89; Fe, 16.46.

Reactions of 3a and 5a with CO under pressure are performed in an autoclave (Berghof Labortechnik GmbH, Tübingen-Lustnau) which allows for drawing samples while the apparatus is under pressure. Solutions of **3a** and **5a**, respectively, in *n*-hexane are pressurized with carbon monoxide. While the temperature is raised to 50 °C (**3a**) or 40 °C (**5a**), samples are drawn in order to monitor the reactions by IR spectroscopy: **3a** is converted into (η^2-*trans*-cyclooctene)Fe(CO)$_4$ while **5a** yields (η^2-diethyl fumarate)Fe(CO)$_4$; the products are identified by comparing the IR spectra with those of authentic samples.

X-ray Structure Determinations of 3a and 5a. Crystals of **3a** (recrystallized from *n*-heptane) and **5a** (recrystallized from *n*-hexane) were mounted in glass capillaries under argon. X-ray data were collected on a Enraf-Nonius CAD-4 diffractometer with graphite-monochromated Mo Kα radiation. Unit-cell data were obtained by a least-squares procedure from 74 reflections ($10.5° < \theta < 23.2°$). Crystallographic data are summarized in Table VIII. Intensity data were collected in the Ω–2θ scan mode with a scan speed of 1–10° min^{-1}. The intensities of three monitor reflections were periodically controlled and showed no significant instability during data collection. The intensity data were corrected for Lorentz and polarization effects, but no correction for absorption was made.

For **3a** the position of the iron atom was determined from a Patterson map, and the rest of the structure was found by a subsequent Fourier synthesis. Refinement was done by full-matrix

least-squares techniques. After anisotropic refinement of the Fe-, C-, and O-atom positions (R = 0.066, R_w = 0.090), it was possible to find all hydrogen atom positions from a difference Fourier calculation. These were included isotropically in the final refinement cycles. Table IX shows the final atomic coordinates; Tables I, II, and III contain selected bond distances, angles, and planes, respectively.

For **5a** the positions of all atoms except hydrogen were found in a Fourier analysis. The positions of hydrogen atoms at C8 and C16 were calculated [d(C–H) = 1.0 Å, U = 0.05], but the other hydrogen atom positions could be taken from a difference Fourier analysis. After an empirical correction for absorption the refinement was carried out by full-matrix least-squares techniques. All non-hydrogen atoms were included anisotropically in the final refinement cycles. Table X shows the final atomic coordinates; Tables VI and VII contain selected bond distances and angles.

Acknowledgment. We are indebted to Mr. K. Schneider and Mrs. R. Schrader for experimental assistance. We thank Dr. W. E. Klotzbücher and Dr. K. Seevogel for IR and ORD/CD measurements, respectively, and Prof. J. Takats for helpful discussions.

Registry No. **2**, 88657-71-0; **3a**, 115224-73-2; [(–)-**3a**], 115224-75-4; **3b**, 115224-76-5; **4**, 65582-71-0; **5a**, 115160-53-7; **5b**, 115224-74-3; **6**, 115160-52-6; (η^2-diethyl formarate)$FeCO_4$, 53150-33-7; (η^2-methyl acrylate)$_2Fe(CO)_3$, 56323-91-2.

Supplementary Material Available: Tables of crystal data and details of data collection, atomic fractional coordinates, atomic thermal parameters, and bond distances and angles for **3a** and **5a** (12 pages); listings of structure factors for **3a** and **5a** (31 pages). Ordering information is given on any current masthead page.

Organometallic Compounds of the Lanthanides. 42.[1] Bis(dimethoxyethane)lithium Bis(cyclopentadienyl)bis(trimethylsilyl)lanthanide Complexes

Herbert Schumann,* Siegbert Nickel, Jörg Loebel, and Joachim Pickardt

Institut für Anorganische und Analytische Chemie der Technischen Universität Berlin, D-1000 Berlin 12, Bundesrepublik Deutschland

Received December 28, 1987

The trichlorides of Sm, Gd, Tb, Dy, Ho, Er, Tm, Yb, and Lu react with NaC_5H_5 in tetrahydrofuran in the presence of dimethoxyethane (dme) with formation of bis(cyclopentadienyl)lanthanide chloride complexes of the types $(C_5H_5)_2Ln(\mu\text{-}Cl)_2Na(dme)$. The reactions of these organolanthanide halide complexes with (trimethylsilyl)lithium in dme yield compounds of the type $[Li(dme)_2][(C_5H_5)_2Ln(SiMe_3)_2]$ (Ln = Sm, Dy, Ho, Er, Tm, Lu). $(C_5H_5)_2Sm(\mu\text{-}Cl)_2Na(dme)$ reacts with (trimethylgermyl)lithium in dme/pentane with formation of $[Li(dme)_3][(C_5H_5)_3SmClSm(C_5H_5)_3]$ (**7a**). The new compounds have been characterized by elemental analyses and IR and NMR spectra. The structure of $[Li(dme)_3][(C_5H_5)_3SmClSm(C_5H_5)_3]$ (**7a**) has been elucidated through complete X-ray analysis. The crystals are monoclinic with a = 14.00 (1) Å, b = 13.38 (2) Å, c = 23.49 (3) Å, β = 93.37 (9)°, space group $P2_1/n$, Z = 4, and R = 0.0411 for 4671 reflections. The $[Cp_3SmClSmCp_3]^-$ anion consists of two Cp_3Sm units bridged by a chlorine atom with Sm–Cl distances of 2.827 (2) and 2.798 (2) Å.

Introduction

Organolanthanides are generally known as hard Lewis acids.[2] Thus the most thermodynamically stable compounds are formed between the lanthanide acceptors and carbon, halogen, or oxygen donors.[3] Only a few examples of organometallic compounds of the lanthanides with bonds to soft donors such as S,[4,5] Se,[6,7] P,[8-13] or As[14] are known. We reported the synthesis of the first bis(cyclopentadienyl)lanthanide triphenylgermyl and triphenylstannyl complexes,[15] and recently we have been successful in synthesizing $[Li(dme)_3][(C_5H_5)_2Sm(SiMe_3)_2]$, the first organometallic compound with a lanthanide to silicon bond.[16] The lanthanide–silicon bond might possess a high degree of "covalency" because of the good donor properties of the trimethylsilyl ligand, although the bonding in organoactinides and organolanthanides is considered to be ionic.[17]

We have investigated the synthesis of the whole series of bis(cyclopentadienyl)bis(trimethylsilyl)lanthanide de-

(1) Part 41: Schumann, H.; Loebel, J.; van der Helm, D.; Hossain, M. B. *Z. Naturforsch., B: Anorg. Chem., Org. Chem.* **1988**, *43B*, 323.
(2) Pearson, R. G. *J. Am. Chem. Soc.* **1963**, *85*, 3533.
(3) For the most recent comprehensive reviews on organolanthanide chemistry see: (a) Schumann, H. *Angew. Chem.* **1984**, *96*, 475; *Angew. Chem., Int. Ed. Engl.* **1984**, *23*, 474. (b) Schumann, H.; Genthe, W. In *Handbook on the Physics and Chemistry of Rare Earths*; Gschneidner, K. A., Eyring, L., Eds.; Elsevier: Amsterdam, 1984; Vol. 7, Chapter 53. (c) Schumann, H. In *Fundamental and Technological Aspects of Organo-f-Element Chemistry*; Marks, T. J., Fragala, I. L., Eds.; D. Reidel: Dordrecht, 1985; pp 1–48. More recent, but more specialized reviews are: (d) Evans, W. J. *Adv. Organomet. Chem.* **1985**, *24*, 131. (e) Kagan, H. B.; Namy, J. L. *Tetrahedron* **1986**, *42*, 6573. (f) Evans, W. J. *Polyhedron* **1987**, *6*, 8003.
(4) Tilley, T. D.; Andersen, R. A.; Zalkin, A.; Templeton, D. H. *Inorg. Chem.* **1982**, *21*, 2644.
(5) Schumann, H.; Albrecht, I.; Hahn, E. *Angew. Chem.* **1985**, *97*, 991; *Angew. Chem., Int. Ed. Engl.* **1985**, *24*, 985.
(6) Schumann, H.; Albrecht, I.; Gallagher, M.; Hahn, E.; Muchmore, Ch.; Pickardt, J. *J. Organomet. Chem.*, in press.
(7) Andersen, R. A., personal communication.
(8) Schumann, H.; Jarosch, H. *Z. Anorg. Allg. Chem.* **1976**, *426*, 127.
(9) Schumann, H.; Frisch, G. M. *Z. Naturforsch., B: Anorg. Chem., Org. Chem.* **1981**, *36B*, 1244.
(10) Bielang, G.; Fischer, R. D. *J. Organomet. Chem.* **1978**, *161*, 335.
(11) Evans, W. J.; Bloom, I.; Hunter, W. E.; Atwood, J. L. *Organometallics* **1983**, *2*, 709.
(12) Schumann, H.; Frisch, G. M. *Z. Naturforsch., B: Anorg. Chem., Org. Chem.* **1979**, *34B*, 748.
(13) Schumann, H.; Palamidis, E.; Schmid, G.; Boese, R. *Angew. Chem.* **1986**, *98*, 726; *Angew. Chem., Int. Ed. Engl.* **1986**, *25*, 718.
(14) Schumann, H.; Frisch, G. M. *Z. Naturforsch., B: Anorg. Chem., Org. Chem.* **1982**, *37B*, 168.
(15) Schumann, H.; Cygon, M. *J. Organomet. Chem.* **1978**, *144*, C43.
(16) Schumann, H.; Nickel, S.; Hahn, E.; Heeg, M. J. *Organometallics* **1985**, *4*, 800.
(17) Raymond, K. N.; Eigenbrodt, C. W. *Acc. Chem. Res.* **1980**, *13*, 276.

0276-7333/88/2307-2004$01.50/0